Journal of proteome research

pubs.acs.org/jpr

Article

Low-Temperature HILIC Provides Enhanced Separations and Stability for LC-MS-Based Metabolomics

Yifan Liu, Madison L. Jastrab, Michael Xiao, Miriam Lisci, Bindu Y. Srinivasu, Taysir K. Bader, Alexis A. Jourdain, Thomas E. Wales, and Owen S. Skinner*

Cite This: https://doi.org/10.1021/acs.jproteome.5c01216

Read Online

ACCESS | Metrics & More | Article Recommendations | Supporting Information

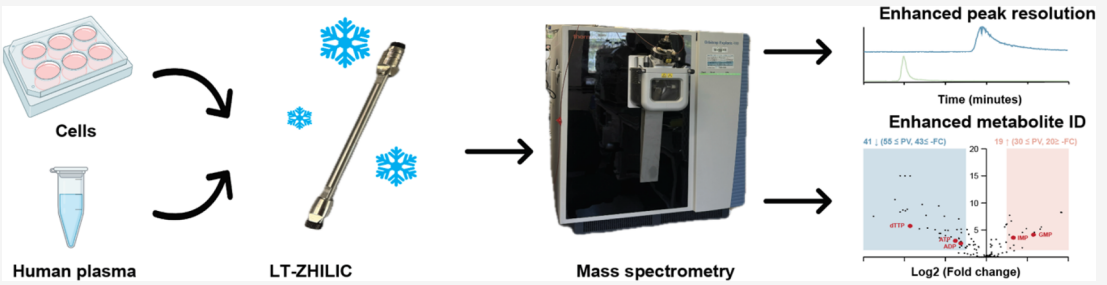

ABSTRACT: Liquid chromatography−mass spectrometry is a potent and robust tool for studying metabolism. However, conventional workflows can suffer from poor peak shapes, limited pressure tolerance, coelution of polar metabolites, and unstable retention times. Here, we describe the development of a more stable HILIC method for LC-MS metabolomics of human plasma and cell extracts, optimizing a zwitterionic HILIC (Z-HILIC) column for improved untargeted performance. We found that using high-pH ammonium bicarbonate with 90% acetonitrile in mobile phase B (ABC B) can greatly improve peak shapes of select metabolites when compared to 100% acetonitrile (ACN B), but at the cost of poor retention time stability. We therefore focused on optimizing chromatography for the ACN B method and observed that cooling the column to 5 °C substantially enhanced peak shape for the BEH-bound Z-HILIC and amide columns but had little effect on the polymeric ZIC-pHILIC column. The low-temperature method with the Z-HILIC column (LT-ZHILIC) enables high-resolution separation of 471 metabolite library standards and from both cellular extracts and human plasma and demonstrates robust stability over 100 consecutive injections and multiple days. Application of the untargeted LT-ZHILIC method to characterize the metabolic consequences of glutamine and pyruvate deficiency in human cells revealed a striking change in nucleotide phosphates—a perturbation that was not observed in the ZIC-pHILIC analysis of the same samples likely due to inadequate elution profiles. In sum, the LT-ZHILIC workflow offers a robust platform to advance untargeted metabolomics by improving metabolite coverage, resolution, and retention time stability, making it a promising technique for providing novel insights into cellular metabolic rewiring and the human plasma metabolome.

KEYWORDS: *HILIC, separation, metabolomics, nucleotides*

INTRODUCTION

Untargeted metabolomics provides a comprehensive and unbiased view of metabolism by profiling a wide range of known and unknown metabolites, making it a beneficial tool to investigate metabolic perturbations and pathway alterations across diverse biological and environmental systems.[1−3] This discovery-oriented approach enables hypothesis generation and the identification of novel biomarkers and pathways, including early metabolic changes in cardiovascular and metabolic diseases. Application of untargeted metabolomics has highlighted the role of the "dark metabolome" in biomarker discovery and uncovered alterations in bile acid, amino acid, and glycan metabolism.[3,4] Of particular interest are polar metabolites like sugars, amino acids, nucleotides, and organic acids, which play central roles in energy metabolism and signaling and whose altered abundances often reflect disease states, drug responses, or nutritional status.[5] However, the chemical diversity, low abundance, and instability of these metabolites make their reliable detection challenging, underscoring the need for robust LC−MS methodologies. Moreover, complex biological samples such as plasma, tissues, and cell extract often generate overlapping signals, adducts, in-source fragments, and isomeric species, all of which further complicate accurate metabolite identification.[6]

Received: December 29, 2025
Revised: May 8, 2026
Accepted: May 22, 2026

Among analytical platforms, LC−MS has proven highly effective due to its superior sensitivity, mass accuracy, and broad metabolite coverage.[7] However, the choice of chromatographic column is critical for accurate metabolite identification. Reverse-phase LC (RP-LC) columns can generate narrow and well-defined chromatographic peak shapes,[8] but very polar and charged compounds are often poorly retained, eluting in an unresolved "void volume" at the start of the chromatogram.[9] This lack of retention hinders separation and increases the likelihood of coelution, especially in complex biological mixtures where metabolites may share similar physicochemical properties, including isomeric forms.[10] To address these challenges, mixed-mode columns that combine reversed-phase and ion-exchange or polar functionalities have been developed to broaden metabolite coverage within a single run.[11] These columns can improve selectivity for compounds with a wide range of polarities, though their dual retention mechanisms often require careful optimization to ensure reproducible separations.

To overcome the limitations of RP-LC for highly polar metabolites, hydrophilic interaction liquid chromatography (HILIC) has emerged as a core strategy in metabolomics. HILIC employs a polar stationary phase and high organic mobile phase, enabling strong retention of charged and hydrophilic compounds such as amino acids, nucleotides, and sugar phosphates that are poorly resolved by RP-LC.[12] This mode of separation is particularly effective for untargeted metabolomics, where comprehensive coverage of central carbon and energy metabolism is critical. Several stationary phase chemistries have been developed, including bare silica, amino, amide and zwitterionic (sulfobetaine) ligands, each providing distinct selectivity through a combination of liquid partitioning, hydrogen bonding, and electrostatic interactions.[13,14] Among zwitterionic HILIC columns, ZIC-pHILIC is one of the most widely used in untargeted metabolomics. It features a polymer ("p") linkage that bonds the sulfobetaine stationary phase to a polymeric support, providing strong retention of highly polar metabolites and broad metabolome coverage, which has made it a standard platform for polar metabolite profiling. However, the polymeric nature of the stationary phase also introduces important limitations. In addition to lower backpressure tolerance (<200 bar) and reduced mechanical robustness compared with hybrid or silica based materials, polymer supports cannot be manufactured in the smaller particle sizes characteristic of UPLC/UHPLC technologies. This constraint limits achievable peak capacity and diminishes the potential gains in sensitivity and resolution, ultimately affecting long-term stability and reproducibility in large-scale metabolomics analyses.[15] To address these weaknesses, one newer design has introduced bridged ethylene hybrid (BEH) particles functionalized with zwitterionic ligands, giving rise to the "Z-HILIC" column.[16] This design provides enhanced mechanical strength and substantially greater pressure tolerance compared with conventional ZIC-pHILIC,[17,18] enabling more robust operation under UHPLC conditions. Separately, both Z-HILIC and ZIC-pHILIC benefit from being packed into inert column hardware, which reduces undesirable metal interactions and protects metal sensitive analytes. Although the mechanisms differ, Z-HILIC uses inert metallic hardware while ZIC-pHILIC employs PEEK-lined material; both approaches help minimize analyte losses associated with metal surfaces.[19] Direct evaluation of the two columns demonstrated that Z-HILIC achieves sharper peak shapes, improved resolution of isomeric species, and greater metabolite coverage than ZIC-pHILIC under similar conditions.[7] However, despite its high promise, certain metabolites remain poorly resolved or exhibit suboptimal peak shapes on Z-HILIC, and the long-term stability of the column under routine use conditions remains insufficiently characterized.

Two main chromatographic approaches have been established for Z-HILIC separations, each offering distinct advantages and compromises. The first method uses 15 mM ammonium bicarbonate at high pH in both mobile phases (ABC B), with mobile phase B consisting of 15 mM ammonium bicarbonate in 90% acetonitrile. This approach provides high efficiency and strong retention of polar analytes particularly for metabolites in central carbon metabolism.[20] In contrast, the second approach uses high-pH ammonium bicarbonate only in mobile phase A with pure acetonitrile as mobile phase B (ACN B), improving the separation and detection of highly polar intermediates and broadening overall metabolite coverage.[21] Despite their widespread use, the relative stability and long-term performance of these two methods have not been systematically evaluated.

Here, we compare both methods and find that the ABC B method, while generally providing better peak shapes than the ACN B method for a broad range of metabolites, exhibits pronounced retention time drift after just 1 day. Although this instability is often overlooked in the metabolomics literature, it poses a significant limitation for large-scale studies that require reproducibility and long-term stability. To address these challenges, we optimized the ACN B method to enhance peak shapes while preserving its superior retention time stability. Through these efforts, we have developed a low-temperature Z-HILIC (LT-ZHILIC) strategy that yielded substantial improvements in peak quality and led to improved chromatographic resolution for metabolites from both human plasma and intracellular extracts. Unlike conventional methods that rely on elevated temperatures to improve peak shapes and reduce tailing, our approach operates at 5 °C, yielding improved separation efficiency while maintaining reproducibility across a wide range of metabolites, including those from cell extracts, plasma, and complex cultured cell metabolomes. We also developed an LT-ZHILIC library comprising 471 metabolites spanning central metabolic pathways, incorporating both retention time and MS/MS information to enable MSI Level 1 metabolite identification.[22] Notably, in untargeted metabolomics of nutrient-deprived cultured cells, unbiased computational analysis detected key intracellular nucleotide phosphates such as ATP, ADP, IMP, and GMP with the LT-ZHILIC method, but not ZIC-pHILIC, highlighting that a robust chromatographic method is essential to capturing biologically relevant metabolic changes under stress. Collectively, our results establish LT-ZHILIC as a robust, high-performance alternative that overcomes the limitations of existing Z-HILIC workflows by combining retention stability with superior chromatographic resolution.

EXPERIMENTAL SECTION

Chemical and LC-MS Reagents

For chromatographic separation, two gradient systems were prepared. The first (ABC B) comprised mobile phase A (15 mM ammonium bicarbonate in MS-grade water; Fisher Scientific) and mobile phase B (15 mM ammonium bicarbonate in 90% acetonitrile; Fisher Scientific), with the pH of mobile phase A adjusted to 9.2 using MS-grade ammonium hydroxide (Fisher Scientific). The second

https://doi.org/10.1021/acs.jproteome.5c01216
J. Proteome Res. XXXX, XXX, XXX−XXX

(ACN B) system used mobile phase A (20 mM ammonium bicarbonate in MS-grade water; Fisher Scientific) and mobile phase B (100% acetonitrile; Fisher Scientific), with the pH of mobile phase A likewise adjusted to 9.2 using MS-grade ammonium hydroxide (Fisher Scientific). The LT-ZHILIC method was initiated at 0.15 mL/min with 80% mobile phase B at 5 °C from 0.0 to 0.5 min. From 0.5 to 20.5 min, the gradient was held at 20% mobile phase B at the same flow rate and maintained until 21.3 min. The column was then equilibrated at 0.15 mL/min and 80% mobile phase B from 21.5 to 26.0 min, followed by a brief flushing step at 0.3 mL/min and 80% mobile phase B from 26.0 to 26.1 min.

Preparation of Cell and Plasma Extractions

K562 cells (purchased from ATCC) were reauthenticated by STR profiling in 2025. Cells were cultured in Dulbecco's Modified Eagle Medium (DMEM; Fisher) supplemented with 10% fetal bovine serum (FBS; Fisher) under standard conditions (37 °C, 5% CO_2). For metabolite extraction, three biological replicates of K562 cells were prepared at a density of 1×10^6 cells/mL in a six-well plate. Each sample was transferred to a microcentrifuge tube and centrifuged at 400 × *g* for 5 min at room temperature, after which the supernatant was carefully aspirated to remove the culture medium. Intracellular metabolites were extracted by adding 600 μL of solvent mixture (40% methanol, 40% acetonitrile, 20% LC−MS-grade water, 240 μL/240 μL/120 μL) containing 0.1 M formic acid. Samples were vortexed briefly and incubated on ice for 10 min. To neutralize the extract, 42 μL of 150 mg/mL ammonium bicarbonate was added to each sample. This extraction strategy was modified from a previously described method.[23]

For plasma metabolite extraction, a mixture containing 40% methanol (MS grade; Fisher), 40% acetonitrile (MS grade; Fisher), and 20% pooled human plasma (Fisher) was prepared to a final volume of 600 μL, vortexed for 10 s, and incubated on ice for 10 min.

Both cell and plasma extracts were centrifuged at 21,000 × *g* for 10 min at 4 °C. The resulting supernatants were transferred to LC vials and analyzed under varying chromatographic conditions, including ammonium bicarbonate (ABC) and acetonitrile (ACN) mobile phases on different HILIC columns.

Untargeted Metabolomics of Glutamine- and Pyruvate-Supplemented K562 Cells

K562 cells (ATCC) were cultured in Dulbecco's Modified Eagle Medium (DMEM; Gibco, A14430-01) supplemented with 25 mM glucose (Sigma, G7021), 2 mM L-glutamine (Amimed, 5-10K00-H), 2 mM sodium pyruvate (Invitrogen, 11360039), 10% fetal bovine serum (FBS; Fisher), and 100 U/mL penicillin−streptomycin (Bioconcept). Cells were maintained under standard conditions (37 °C, 5% CO_2) in T25 or T75 flasks and subjected to four treatment conditions: (+Gln/+Pyr), (+Gln/−Pyr), (−Gln/+Pyr), and (−Gln/−Pyr). For nutrient-deprivation conditions, water was substituted for the omitted component. K562 cells were seeded at 0.5×10^6 cells/mL for + glutamine conditions (12.5×10^6 cells in 25 mL) or 0.6×10^6 cells/mL for − glutamine conditions (15×10^6 cells in 25 mL) and cultured in T75 flasks at 37 °C with 5% CO_2 overnight. The following day, 20×10^6 cells from each condition were collected, resuspended in 40 mL of freshly prepared medium, and split into four T25 flasks (10 mL each) as technical replicates. After 5 h of incubation, cells were harvested by centrifugation at 300 × *g* for 3 min, washed once with PBS, and flash frozen in liquid nitrogen for metabolite extraction. The extraction procedure was the same as nontreated K562 cells mentioned previously. This research did not involve human or animal participants.

Instrumentation (LC-MS Analysis and Cryogenic LT-ZHILIC Setup)

Samples were maintained at 4 °C in the autosampler before analysis. LC−MS experiments were performed on a Vanquish UHPLC system coupled to an Orbitrap Exploris 480 mass spectrometer (Thermo Fisher Scientific). In parallel, additional experiments were conducted using an M-Class ACQUITY UPLC system coupled to a SYNAPT G2-Si mass spectrometer (Waters). For the cryogenic experiments, the column was cooled to −20 °C using a thermoelectric temperature controller (TC-48-20; TE Technology). Chromatographic separations were performed using a Waters Premier BEH Z-HILIC column (1.7 μm, 2.1 × 150 mm; item no. 186009983) equipped with a matching VanGuard precolumn (1.7 μm, 2.1 × 5 mm; item no. 186009984). For comparison, the same LC−MS setup was used with a ZIC-pHILIC column (2.1 × 150 mm; Sigma-Aldrich, item no. 1.50460.0001) and a Waters BEH Amide column (1.7 μm, 2.1 × 100 mm; item no. 186009932), also equipped with a matching VanGuard precolumn. Column temperature was varied according to method conditions to evaluate chromatographic performance.

Modified chromatographic conditions are described in Table 1. The original ABC B LC method was operated at a flow rate of 0.30 mL/min, with the column temperature set to 30 °C and the initial mobile phase B composition at 90%. The original ACN B method was run at a flow rate of 0.15 mL min^{-1}, with the column temperature maintained at 30 °C and the initial mobile phase B composition at 80%. The optimized LT-ZHILIC method was operated at a flow rate of 0.15 mL min^{-1}, a column temperature of 5 °C, and a starting mobile phase B composition of 80%. The mass spectrometer was operated at a resolution of 60,000 with a scan range of m/z 70−1000 in polarity switching mode (positive and negative). The H-ESI ion source was used with static spray voltages of +3.2 kV (positive) and −2.8 kV (negative). Gas settings were fixed: sheath gas = 35, auxiliary gas = 5, sweep gas = 1, ion-transfer tube temperature = 320 °C, and vaporizer temperature = 175 °C. For comparable experiments performed using the Waters instrument, the flow rate was adjusted to 0.1 mL min^{-1}, and the chamber temperature was maintained at 5 °C. The SYNAPT G2-Si mass spectrometer was operated in negative ion mode. For MS/MS fragmentation, negative and positive modes were acquired separately using the AcquireX Deep Scan workflow. In negative mode, the intensity threshold was set to 5×10^4, with dynamic exclusion enabled after one occurrence, an exclusion duration of 15 s, and a mass tolerance of 10 ppm.

Table 1. Summary of Key Method Parameters for Chromatographic Optimization[a]

method name	flow rate (mL/min)	temperature (°C)	initial B%
M0	0.15	30	80
M1	0.3	30	80
M2	0.15	30	95
M3	0.15	50	80
M4	0.15	10	80
M5	0.1	10	80
M6	0.15	10	85
M7	0.15	10	90
M8	0.15	10	95
M9	0.15	5	80

[a]A series of methods (M0−M9; Table 1) were developed by systematically varying flow rate, column temperature, and initial mobile phase B composition. The baseline method (M0) employed 80% initial mobile phase B, a flow rate of 0.15 mL min^{-1}, and a column temperature of 30 °C. The final optimized method (M9) was used for further experiments.

Cryogenic temperature experiments were conducted by enclosing the Z-HILIC column in a custom insulated foam housing connected to an external refrigerated chamber.[24] This setup was required because the UHPLC column compartment could not be operated below 4 °C. The chamber was maintained at various subzero temperatures (<0 °C) and directly coupled to the LC−MS system to ensure stable low-temperature operation.

Data Processing and Metabolite Identification (Freestyle and Compound Discoverer)

Metabolite profiles from each replicate were analyzed using Freestyle (Thermo Fisher Scientific) to evaluate peak shapes. For experiments

https://doi.org/10.1021/acs.jproteome.5c01216
J. Proteome Res. XXXX, XXX, XXX−XXX

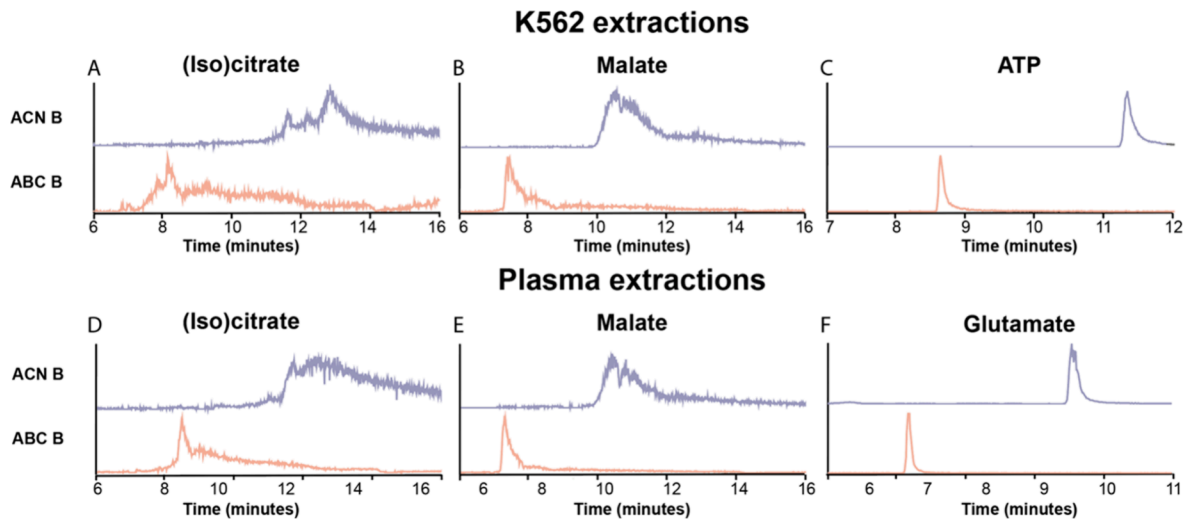

Figure 1. Metabolite peak shape comparison between ACN B and ABC B. (A–F) Representative chromatograms of selected metabolites, (iso)citrate, malate, and ATP in K562 cell extracts (A–C) and (iso)citrate, malate, and glutamate for plasma samples (D–F) run using the ACN B (purple) and ABC B (orange) methods (n = 2 replicates for ABC B, n = 3 replicates for ACN B). Method details are described in the Experimental Section.

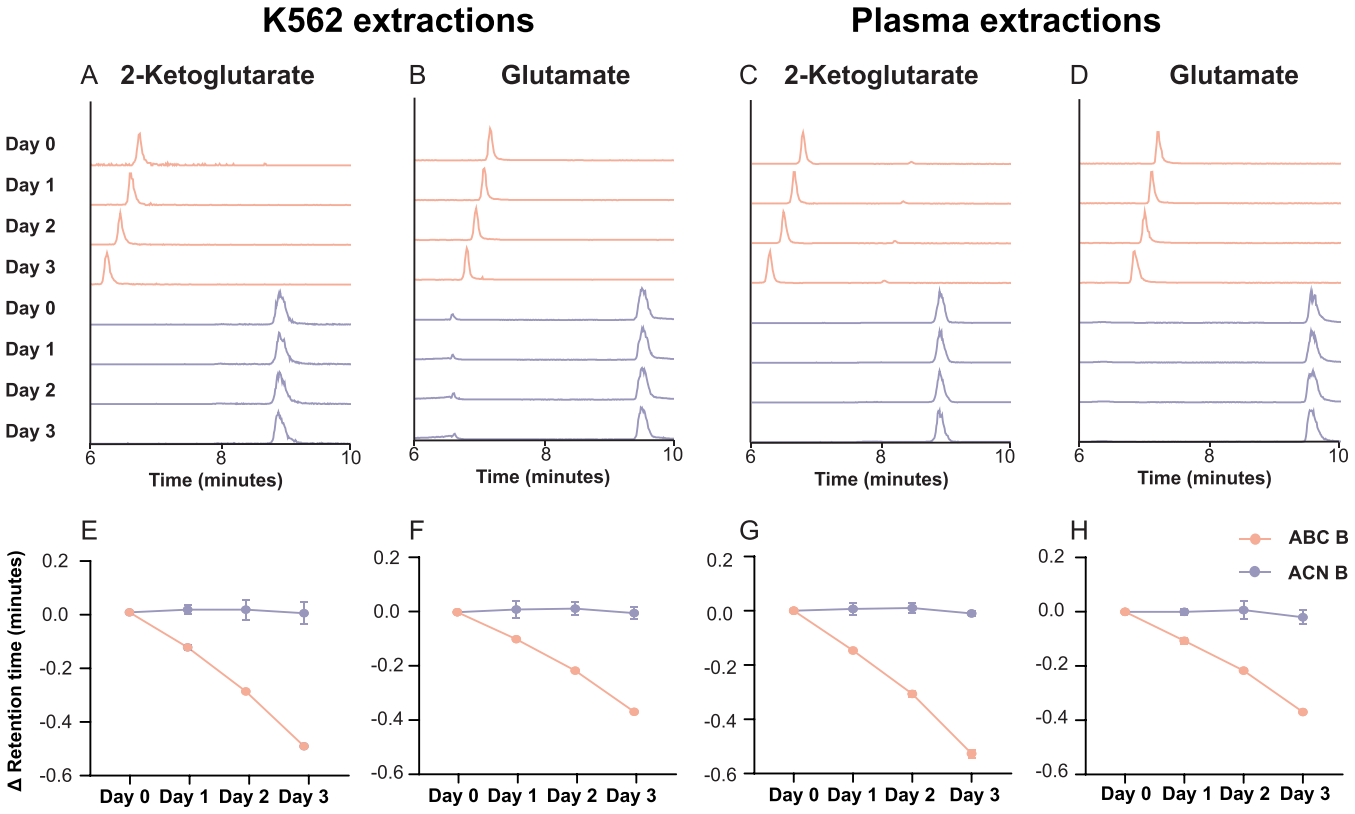

Figure 2. Retention time stability of ABC B and ACN B. (A–D) Representative chromatograms of 2-ketoglutarate and glutamate in K562 cell extracts (A, B) and plasma samples (C, D) over 4 days (n = 2 replicates for ABC B, n = 3 replicates for ACN B). Metabolites analyzed using the ABC B method are shown in orange; those analyzed using the ACN B method are shown in purple. (E–H) Change in retention time for each metabolite over a 4 days' time course (day 0 to day 3) comparing the ABC B (orange) and ACN B (purple) methods.

performed on the Waters system, metabolite identification was conducted using MassLynx. Chromatograms shown in the representative figures were smoothed (10) and baseline corrected (subtract 1). Four representative metabolites, (iso)citrate, malate, ATP, and glutamate, were selected for peak shape comparison, and their chromatograms were extracted directly from Freestyle. Retention time comparisons were performed in Skyline (University of Washington). A transition list for key metabolites, including 2-ketoglutarate, glutamate, and succinate, was manually generated based on their precursor m/z values, using $[M - H]^-$ as the precursor ion for negative mode detection. Retention time data were exported from Skyline and analyzed in Prism (GraphPad) to calculate mean values and standard deviations.[1]

For comprehensive metabolite identification, cultured cell extracts were analyzed using both ZIC-pHILIC and LT-ZHILIC methods, followed by pooled sample analysis with an AcquireX deep-scan

https://doi.org/10.1021/acs.jproteome.5c01216
J. Proteome Res. XXXX, XXX, XXX–XXX

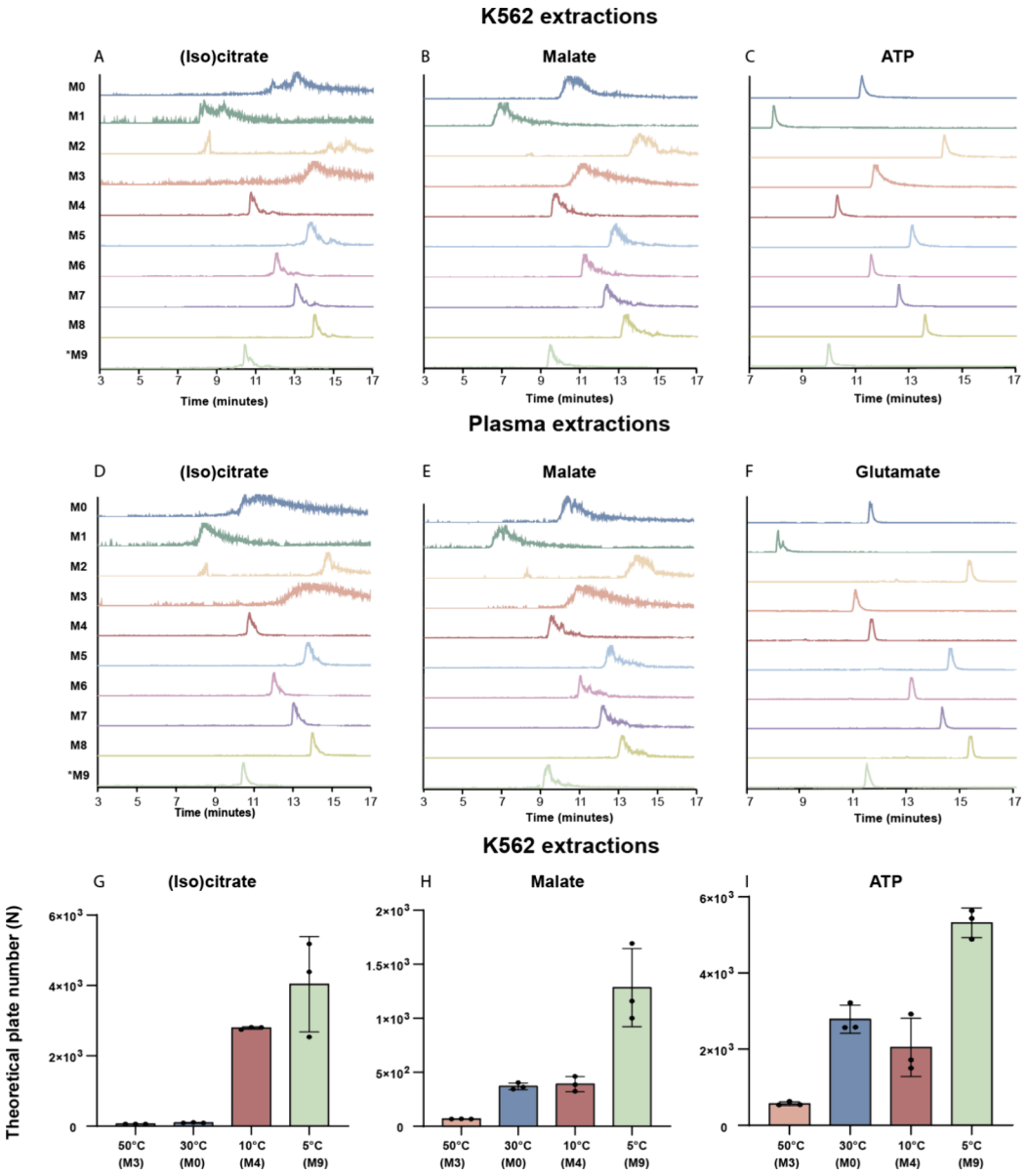

Figure 3. Optimization of the ACN B method using the parameter sets (M0−M9) described in Table 1. (A−C) Representative chromatograms of (iso)citrate, malate, and ATP in K562 cell extracts. (D−F) Corresponding chromatograms of (iso)citrate, malate, and glutamate in plasma samples (n = 3 replicates per method). M0 represents the baseline ACN B method, employing a flow rate of 0.15 mL/min, a column temperature of 30 °C, and an initial composition of 80% mobile phase B. The parameters for each subsequent optimization step are summarized in Table 1. The final optimized method (M9), using a flow rate of 0.15 mL/min, a column temperature of 5 °C, and an initial 80% B, provided the best overall peak performance and is hereafter referred to as LT-ZHILIC. (G−I) Representative theoretical plate number (N) calculations for selected metabolites extracted from K562 cells, comparing methods that differ exclusively in column temperature.

workflow in Xcalibur (Thermo Fisher Scientific) to obtain MS/MS spectra. The resulting data were processed in Compound Discoverer (Thermo Fisher Scientific) using the following filters: matched MS/MS spectra, nonblank compound names, correct reference ion polarity (+ for positive mode, − for negative mode), peak rating ≥7, and mzCloud best-match score ≥50. Compound identification employed a four-tiered library search strategy encompassing mzCloud, predicted compound matches, mass-list searches, ChemSpider, and Metabolika databases. Volcano plots were generated in Prism for statistical and comparative visualization of differential metabolite features. An in-house LT-ZHILIC library was generated using the Mass Spectrometry Metabolite Library of Standards (MSMLS) purchased from IROA Technologies, a collection of ∼600 high-purity small biochemical molecules spanning a broad range of primary metabolism. Metabolites were manually annotated by matching retention times and further evaluated in Compound Discoverer through searches against online spectral libraries. Statistical significance between groups was determined using a two-tailed Student's t test, with significance thresholds set at $^{*}p < 0.05$, $^{**}p < 0.01$, and $^{***}p < 0.001$.

RESULTS

Comparing the ABC B and ACN B Gradient Systems

To evaluate the performance of the Z-HILIC column for untargeted metabolomics, we applied the ABC B and ACN B methods to two representative biological matrices: intracellular metabolites isolated from K562 human myelogenous leukemia cells and circulating metabolites from human plasma. We selected (iso)citrate, malate, and ATP (K562) or glutamate (plasma), which exhibited distinct elution profiles that allowed

https://doi.org/10.1021/acs.jproteome.5c01216
J. Proteome Res. XXXX, XXX, XXX−XXX

us to directly evaluate the performance of each method (Figure 1. In cell extracts, (iso)citrate showed comparable elution profiles between the ABC B method (orange traces) and the ACN B method (purple traces) (Figure 1A), whereas malate and ATP displayed sharper and more symmetrical peaks with the ABC B method (Figure 1B,C). Similar improvements in peak shape were observed for other metabolites in plasma samples (Figure 1D−F). These results indicate that the ABC B method produced sharper elution profiles for the selected metabolites in both plasma and intracellular extracts. Notably, malate in K562 cells showed the largest improvement, with the full peak width decreasing from 2.28 ± 0.08 min under the ACN B method to 1.21 ± 0.42 min using ABC B (Figure 1B).

We next characterized the retention time stability of each method across multiple days, a critical characteristic for the successful analysis of large batches of samples that is common practice for metabolomics workflows. We conducted a 4-day time course experiment to evaluate the stability of ABC B and ACN B mobile phase B systems. We evaluated glutamate, alpha-ketoglutarate, and succinate due to their consistently well-resolved elution profiles with both separation in both cell extracts (Figure 2A,B,E,F andFigure S1A,B) and plasma extracts (Figure 2C,D,G,H andFigure S1C,D) to monitor retention time precision. With ABC B (orange traces), the retention time of the 2-ketoglutarate peak from cell extracts progressively shifted from 6.79 ± 0.01 to 6.30 ± 0.01 min from day 0 to day 3 (Figure 2A). A previous report suggested that glass solvent bottles can affect retention time due to leaching; however, the shift we observed was not corrected by using high-density polyethylene plastic solvent bottles (Figure S1E,F).[25] The corresponding ΔRT plots further emphasized this observation: ABC B exhibited an average retention time drift of ∼0.5 min by day 3 relative to day 0 of all three replicates of 2-ketoglutarate, whereas ACN B showed minimal deviation (<0.01 min) across the 4-day period (Figure 2E,F). Similar patterns were observed for glutamate in both cell and plasma extracts (Figure 2C,D,G,H). Collectively, our results demonstrate that while ABC B results in improved peak shapes, it suffers from severe retention time drift that does not affect ACN B, suggesting that ACN B has better performance for larger sample batches.

Optimization of ACN B Chromatography

The ACN B method maintained stable retention times but yielded suboptimal peak shapes, primarily due to significant tailing, most notably for (iso)citrate and malate (Figure 1). To systematically address these limitations, we optimized chromatographic conditions by varying flow rate, column temperature, and the initial percentage of mobile phase B, generating a series of methods described in Table 1(M0−M9). The original ACN B protocol (M0, Figures 1 and 2), which uses 80% initial mobile phase B, a flow rate of 0.15 mL/min, and a column temperature of 30 °C, M0, served as the baseline condition. We used the (iso)citrate, malate, and ATP or glutamate from intracellular and plasma extracts (as in Figure 1) to assess changes in peak quality. Increasing the flow rate to 0.3 mL/min (M1) yielded little improvement; (iso)citrate peaks remained jagged and poorly resolved (Figure 3A). Similarly, raising the initial mobile phase B to 95% (M2) did not improve peak symmetry and introduced unrelated background peaks. Consistent with prior reports,[7] column temperature adjustments had more pronounced effects. Increasing the temperature to 50 °C (M3) improved peak quality for ATP in cell extracts and glutamate in plasma extracts (Figure 3C,F), though (iso)citrate and malate continued to display broad, tailing peaks. Decreasing the temperature to 10 °C (M4) improved chromatographic performance across these metabolites, yielding more symmetrical peaks. Building on this observation, we tested additional refinements of flow rate and mobile phase composition (M5−M8) under low-temperature conditions but observed only modest benefits, as (iso)citrate and malate peaks remained broad and jagged. The final optimized method (M9), employing 80% mobile phase B, a flow rate of 0.15 mL/min, and a column temperature of 5 °C, delivered the best overall targeted analysis. This method, which we termed "low-temperature Z-HILIC" or LT-ZHILIC, produced consistently narrow peak widths and improved peak symmetry for all tested metabolites, with notable improvements in (iso)citrate and malate peak shapes (Figure 3A,B,D,E; light green traces). Theoretical plate numbers (N) were calculated for selected metabolites in K562 cell extracts using methods M0, M3, M4, and M9 to quantify the chromatographic improvements attributable to column temperature differences (Figure 3G−I). At equivalent flow rates and initial mobile phase B compositions, the 5 °C method (M9) yielded the highest N values, indicating superior peak performance, while the high-temperature method (50 °C) produced the lowest N values. Interestingly, all three of these selected compounds exhibited earlier retention times at colder temperatures. Collectively, our results demonstrate that lowering the column temperature is an effective strategy for improving peak shape in the ACN B method, establishing LT-ZHILIC as a robust method for metabolomics applications.

Building on the low-temperature results, we next examined whether further cooling could enhance chromatographic separation. To this end, we maintained the Z-HILIC column under cryogenic conditions, with temperatures lowered to −20 °C using a custom-designed temperature-controlled chamber to assess performance stability and peak resolution (Figure S2A−D). We analyzed the same representative metabolites from both intracellular and plasma extracts for direct peak-shape comparison (Figure S3A−F). Relative to the LT-ZHILIC method at 5 °C (light-green traces), further reductions in temperature (−5, −10, and −20 °C; darker-green traces, top to bottom) did not yield improvements. In fact, at −10 °C, peak shapes deteriorated noticeably, for example (iso)citrate in cell extractions (Figure S3A). These findings indicate that the optimal performance is achieved with the LT-ZHILIC method at 5 °C, while lower cryogenic temperatures compromise chromatographic quality.

To confirm that the LT-ZHILIC method exhibits retention time stability comparable to ACN B, we evaluated its performance in both 4-day and 11-day time course experiments (Figures S4A−H and S5A−H). As in the previous analysis (Figure 2), 2-ketoglutarate and glutamate were selected as representative metabolites (Figure S4A−H). Chromatograms of 2-ketoglutarate from cell extracts collected over days 0−3 showed minimal retention time drift, with ΔRT values below 0.023 min (Figure S4A,E). Similar stability was observed for additional metabolites in both cell and plasma extracts, with negligible ΔRT values maintained throughout the 4-day period (Figures S4B−D,F−H and S5A,B,E,F). To assess longer-term stability, we extended the analysis to an 11-day time course using plasma extracts (Figure S5C,D,G,H). 2-Ketoglutarate exhibited a retention time drift of only 0.08 ±

https://doi.org/10.1021/acs.jproteome.5c01216
J. Proteome Res. XXXX, XXX, XXX−XXX

0.01 min over the entire period (Figure S4C,G), indicating robust retention time reproducibility. Chromatographic performance and ΔRT values remained consistent throughout the 11 days' analysis. Collectively, these results demonstrate that LT-ZHILIC improves chromatographic performance while maintaining stable retention times over extended analytical sequences. This level of stability is critical for large-scale metabolomics studies, where minimizing retention time drift ensures reliable feature alignment, preserves metabolite detectability, and enables consistent comparisons across large sample cohorts.

Building on the demonstrated stability of LT-ZHILIC, we analyzed over 600 small-molecule metabolites (IROA Technologies) spanning major metabolic pathways, acquiring both MS^1 and MS/MS data in negative and positive ion modes using AcquireX (Thermo). In total, 405 metabolites were identified in negative ion mode and 331 in positive ion mode, each supported by MS^1 and MS^2 spectral evidence, yielding 471 unique metabolites across both modes combined. Metabolites with multiple possible retention times are indicated by (1), (2), etc. We compiled these data into a comprehensive LT-ZHILIC library integrating retention time and MS/MS spectra (Figure 4A). Metabolites identified in each ionization mode were further classified by chemical class, as summarized in the corresponding bar plots (Figure 4B,C). This LT-ZHILIC library enables MSI level 1 confidence in metabolite identification and was subsequently applied in the following analyses.

To further evaluate the stability of LT-ZHILIC for large-scale analyses, we performed 100 consecutive injections of plasma extracts and conducted metabolite identification and annotation against the LT-ZHILIC library (Figure 5A–J andFigure S6A–D). This experiment was carried out using a Z-HILIC column coupled with an integrated guard column, which was not replaced throughout the study. The peak shapes of selected metabolites, such as (iso)citrate, remained consistently sharp and symmetric across injections (e.g., injections 1, 30, 60, and 100; Figure 5A). Retention times were highly stable, with (iso)citrate exhibiting a drift of less than 0.04 min over 100 injections (Figure 5C). Similar trends were observed for malate (Figure 5B,D), demonstrating excellent reproducibility during continuous large batch analyses. The LT-ZHILIC maximum back pressure exhibited a variation of <2% between the 1st and 100th injections, indicating stable performance under low-temperature conditions during consecutive analyses (Figure S6E).

We next applied the LT-ZHILIC library to assess peak area and base peak width stability across repeated injections. We identified 83 metabolites in negative mode and 43 metabolites in positive mode (Figure 5E). Identified metabolites spanned across a wide range of biologically active molecule classes (Figure 5F). Peak area reproducibility was evaluated by comparing injections 1 vs 2 and 1 vs 100 in both modes (Figure 5G,H andFigure S6A,B). Strong linear correlations were observed between injections 1 and 2, as well as between injections 1 and 100, indicating stable peak intensity across the analytical sequence (Figure 5G,H). Consistent trends were also observed in positive ion mode (Figure S6A,B). The consistent distribution of base peak widths for identified metabolites in each ionization mode further demonstrates the reproducibility of LT-ZHILIC (Figure 5I,J andFigure S6C,D). Together, these results demonstrate the excellent analytical stability of LT-ZHILIC, particularly within a 0.2 min retention time window, corresponding to MSI level 3 identification confidence.

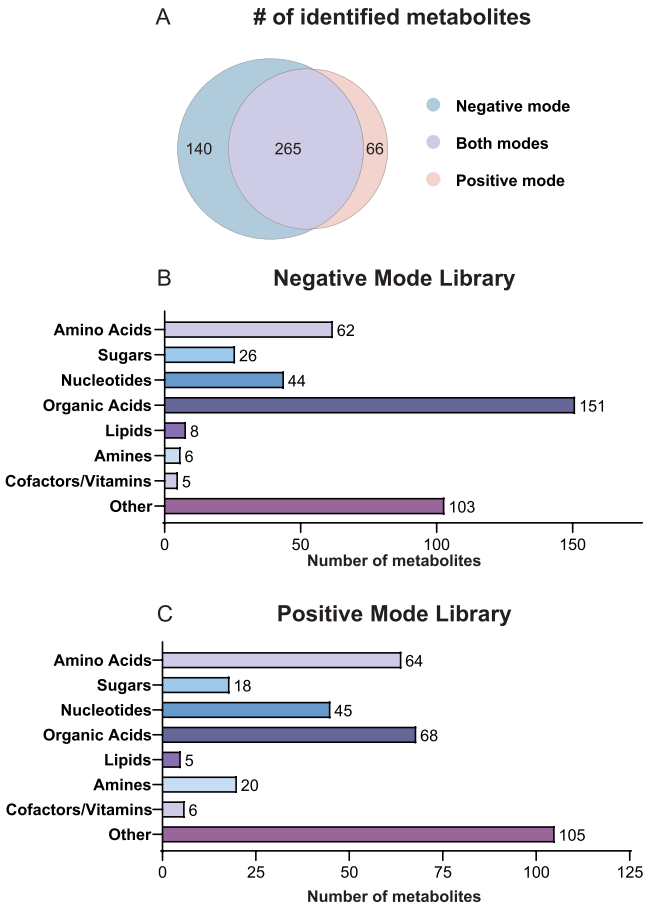

Figure 4. Distribution of metabolite classes identified using the LT-ZHILIC library in both negative and positive ionization modes. Amino acids, sugars, nucleotides, organic acids, lipids, amines, cofactors/vitamins, and other metabolites were identified based on matched retention times and MS/MS spectra. (A) Summary of metabolite identifications across ionization modes, including metabolites detected exclusively in negative mode, exclusively in positive mode, and in both modes. (B) Distribution of metabolite classes identified in negative ion mode. (C) Distribution of metabolite classes identified in positive ion mode.

To assess the transferability of this method across different LC-MS platforms, we performed additional experiments using an M-Class ACQUITY UPLC system coupled to a SYNAPT G2-Si mass spectrometer (Waters) (Figure S7A–C).

Due to flow rate limitations of the M-Class system, the method was operated at 0.1 mL min^{-1} instead of 0.15 mL min^{-1} used in the original LT-ZHILIC configuration. Consistent with observations from the Thermo system, low-temperature conditions (light-green traces) produced narrower peaks compared to room-temperature operation (yellow traces), although the improvement was more subtle. For example, (iso)citrate showed a reduction in peak width of 0.50 ± 0.09 min under low-temperature conditions (Figure S7A). In addition, malate, which was partially split under room-temperature conditions, exhibited improved resolution at low temperature (Figure S7B). Although some peak tailing was observed, this likely reflects differences in LC configuration and the reduced flow rate of the M-class ACQUITY system. Collectively, these results demonstrate that the advantages of

https://doi.org/10.1021/acs.jproteome.5c01216
J. Proteome Res. XXXX, XXX, XXX−XXX

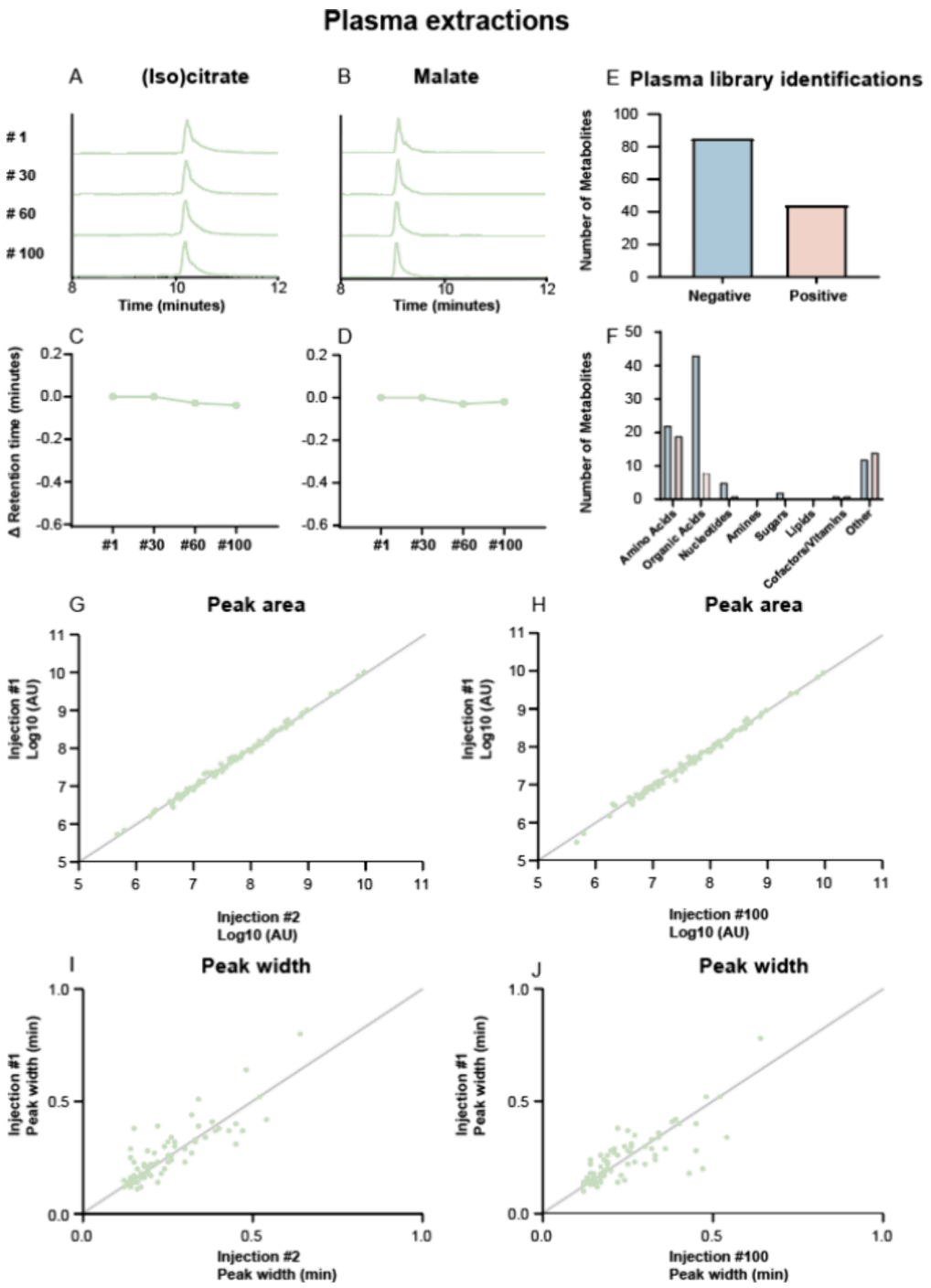

Figure 5. Evaluation of LT-ZHILIC performance across 100 consecutive injections of plasma extracts. (A, B) Representative chromatograms of (iso)citrate (A) and malate (B), illustrating retention time stability over 100 injections. (C, D) Retention time drift (ΔRT) across 100 injections, highlighting selected injections (1, 30, 60, and 100) for (C) (iso)citrate and (D) malate. (E) Number of metabolites identified in negative and positive ion modes against the LT-ZHILIC library at MSI level 3 confidence (retention time matching). (F) Distribution of annotated metabolites (MSI level 3) across chemical classes. (G–J) Comparison of peak area and peak width across multiple injections, with all library-identified metabolites from negative ion mode. (G, H) Representative comparisons of peak area for plasma extract injections 1, 2, and 100. (I, J) Corresponding comparisons of base peak width for injections 1, 2, and 100.

LT-ZHILIC are reproducible across different LC-MS platforms, supporting the broader applicability of this approach.

Comparison of ZIC-pHILIC and LT-ZHILIC Performance

We next compared the LT-ZHILIC method to an established method on the ZIC-pHILIC column (Figure S8A–F).[21,26] In cell extracts, (iso)citrate exhibited comparable peak symmetry and sharpness between ZIC-pHILIC (blue trace) and LT-ZHILIC (light-green trace) (Figure 6A). Similarly, other metabolites showed consistent peak symmetry and sharpness across both columns in cell and plasma extracts (Figure S8B–F). Notably, ATP exhibited sharper and narrower peaks under LT-ZHILIC conditions, highlighting its improved chromatographic performance. These findings indicate that LT-ZHILIC achieves peak shapes equivalent to, and in some cases

https://doi.org/10.1021/acs.jproteome.5c01216
J. Proteome Res. XXXX, XXX, XXX−XXX

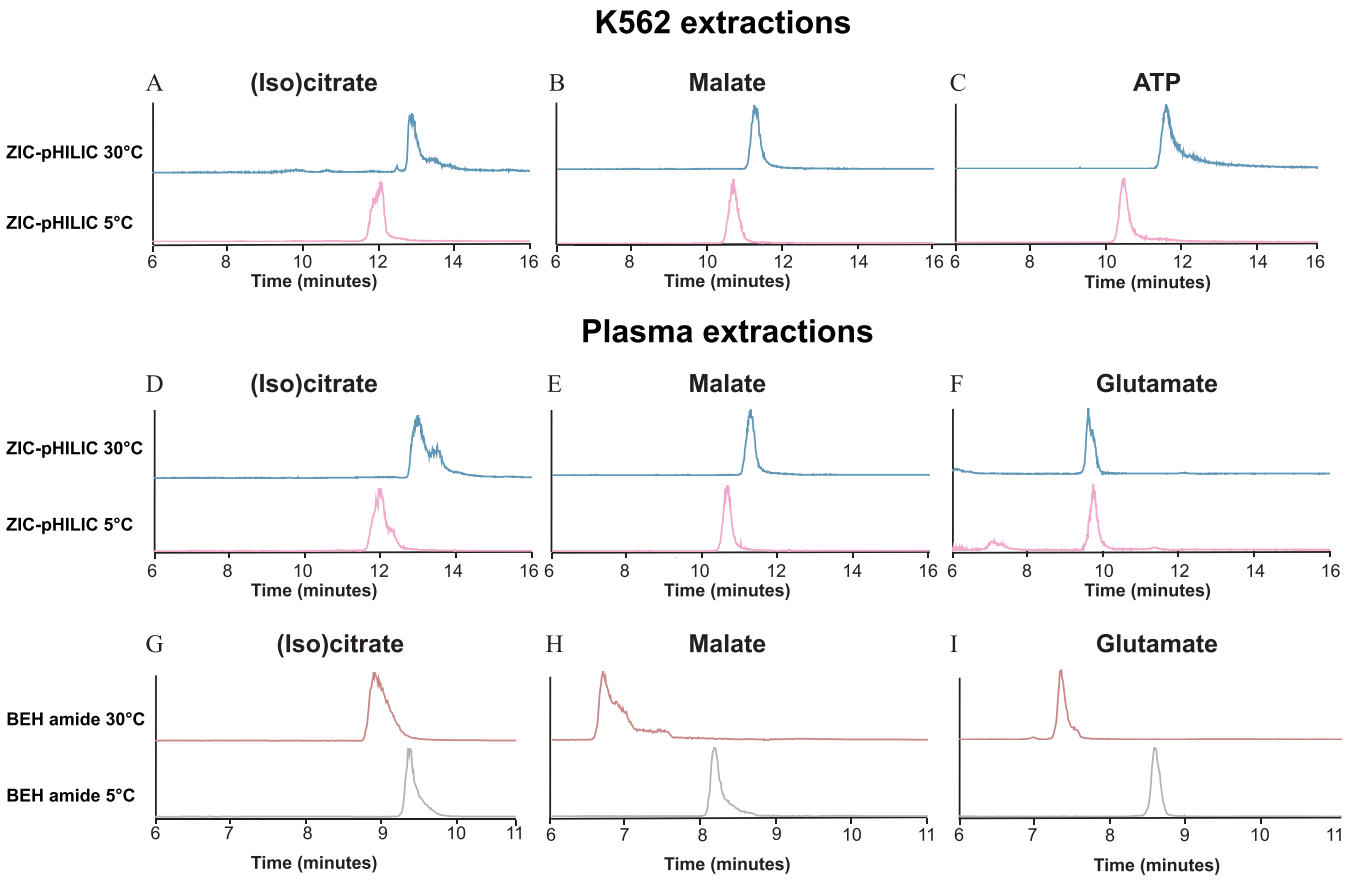

Figure 6. Peak shape comparison of selected metabolites analyzed on ZIC-pHILIC and BEH Amide columns under different temperature conditions. Representative chromatograms from K562 cell extracts (A–C) and corresponding plasma extracts (D–F) acquired on the ZIC-pHILIC column, as well as plasma extracts analyzed on the BEH Amide column (G–I). For ZIC-pHILIC, traces acquired at 30 and 5 °C are shown in blue and pink, respectively. For the BEH Amide column, traces acquired at 30 and 5 °C are shown in red and gray, respectively.

surpassing, that of the ZIC-pHILIC column, underscoring its potential as a robust alternative for metabolomics applications. Given the peak shape improvement with using the Z-HILIC column at low temperature, we next applied the low-temperature strategy to ZIC-pHILIC at 5 °C to test whether performance could be further improved (Figure 6A–F). In K562 extracts, (iso)citrate showed no improvement compared to the original ZIC-pHILIC method at 30 °C (blue traces); the 5 °C ZIC-pHILIC runs (pink traces) even produced less symmetrical peaks with more tailing (Figure 6A). Other metabolites similarly showed no enhancement with the low-temperature approach. For instance, glutamate displayed an unrelated small peak eluting at an earlier retention time in the 5 °C ZIC-pHILIC method (Figure 6F). Notably, these metabolites still eluted earlier at cold temperatures. Overall, these results indicate that the benefits of the low-temperature strategy do not translate to ZIC-pHILIC. We therefore used ZIC-pHILIC at 30 °C for the further performance comparisons.

Given the similar BEH particles chemistry shared by Z-HILIC and BEH Amide columns, we next evaluated whether the low-temperature strategy could be extended to the BEH Amide column applied to plasma extracts (Figure 6G–I). The LT-ZHILIC method was applied under identical conditions on the BEH Amide column. In contrast to ZIC-pHILIC, lowering the column temperature from 30 °C (red traces) to 5 °C (gray traces) resulted in improved peak performance for selected metabolites. In particular, (iso)citrate and malate exhibited sharper and more symmetrical peak shapes at 5 °C (Figure 6G,H), while glutamate showed a more modest improvement (Figure 6I). In contrast to the Z-HILIC and ZIC-pHILIC columns, low temperature increased retention times of select metabolites. More broadly, these results suggest that operating at low temperatures may improve peak shapes for other HILIC stationary phases, especially those using BEH stationary phases.

To investigate mechanistically why low temperature improves chromatographic separation including the contributions of buffer partitioning and column temperature, we characterized how different temperature conditions applied to both the column and mobile phase affect the separation performance of the Z-HILIC column (Figure S9A–F). Consistent with previous experiments, chromatograms obtained under cold column conditions (Figure S9A–C) exhibited narrower and more symmetrical peaks compared with those obtained under warmer column conditions (Figure S9D,E). Using ice-cold mobile phase (brown traces) also produced slightly narrower peaks, particularly for (iso) citrate and glutamate (Figure S9A,C). These results suggest that maintaining the solvents and column cold is the primary factor driving improved chromatographic performance, and not the temperature differential between warm solvents and cold column.

https://doi.org/10.1021/acs.jproteome.5c01216
J. Proteome Res. XXXX, XXX, XXX–XXX

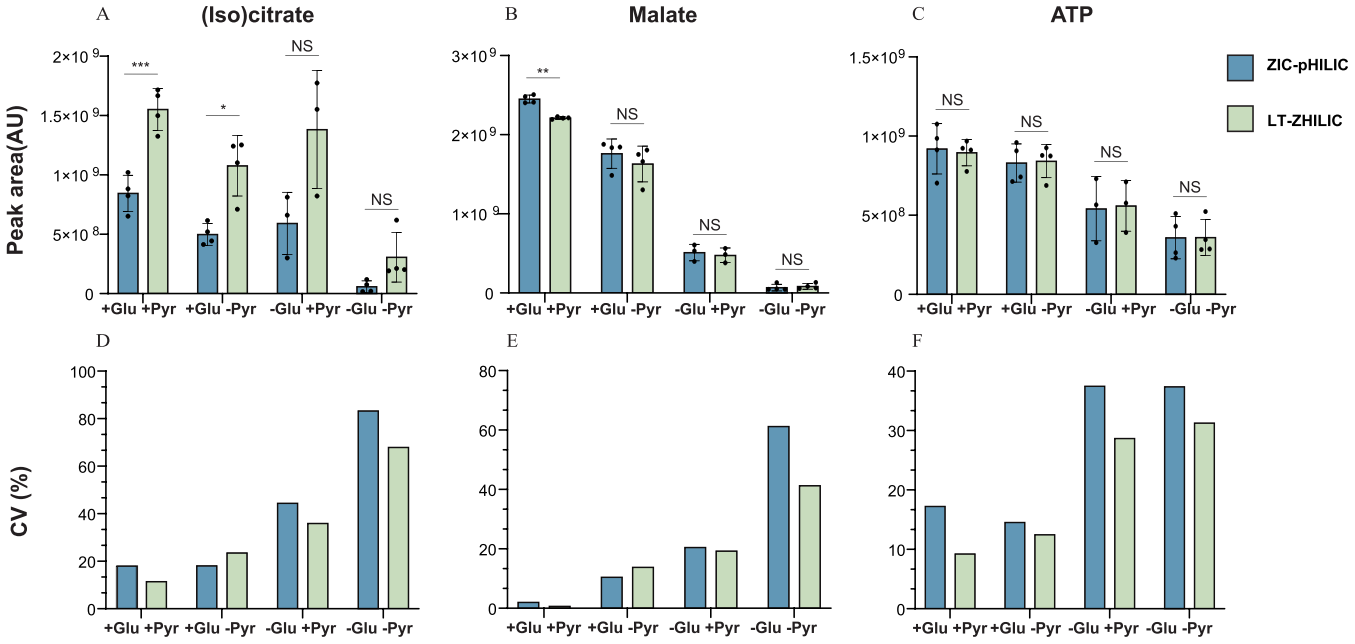

Figure 7. LT-ZHILIC vs ZIC-pHILIC quantitation of selected metabolites in cells with nutrient deficiency. (A–F) Comparison of peak areas across from K562 cells with four treatment conditions analyzed on ZIC-pHILIC (blue) and LT-ZHILIC (green), comparing the sensitivity of both methods for treated biological samples (A–C) and coefficient of variation (CV%) analysis of both methods for each group (D–F).

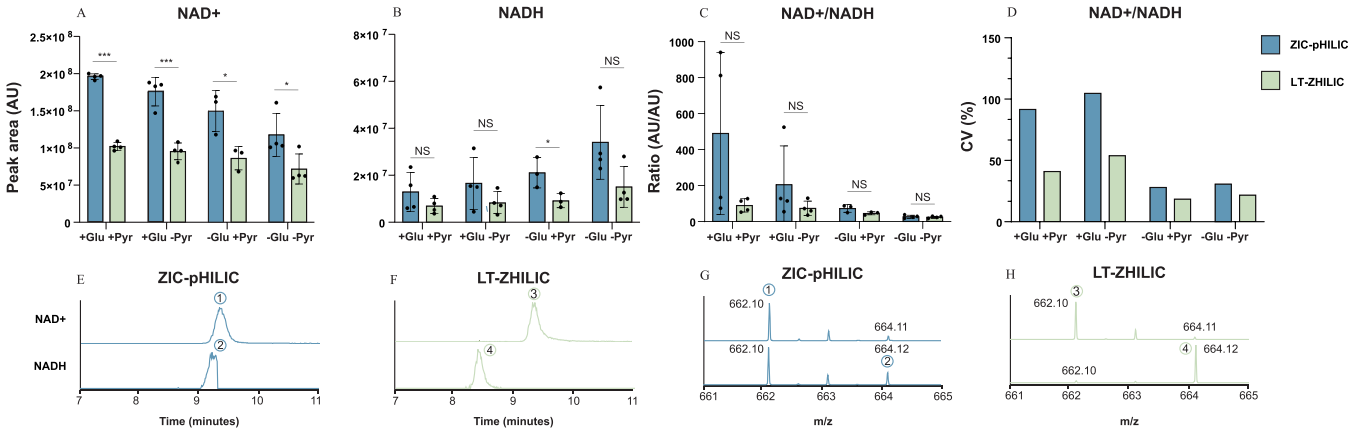

Figure 8. Targeted quantitation of NAD+ and NADH redox cofactors. (A–C) Peak areas of NAD^+, NADH, and NAD^+/NADH in K562 cell extracts analyzed using ZIC-pHILIC (blue) and LT-ZHILIC (green). (D) Coefficient of variation (CV%) for NAD^+/NADH under both methods. NAD^+ and NADH coelute on ZIC-pHILIC, whereas LT-ZHILIC achieves clear baseline separation (E, F), with peak identities indicated. Corresponding mass spectra (G, H) show overlapping signals in ZIC-pHILIC and distinct spectral resolution in LT-ZHILIC, with aligned peak annotations.

Targeted Metabolomics Analysis of Cultured Cell Extracts Using LT-ZHILIC

To further evaluate the performance of the LT-ZHILIC method in complex biological samples, we cultured K562 cells under four nutrient conditions varying in glutamine and pyruvate availability: (1) complete medium containing both substrates (control), (2) glutamine only, (3) pyruvate only, and (4) medium lacking both glutamine and pyruvate. Each nutrient condition was analyzed with four biological replicates ($N = 4$) in the single-cell culture experiment. We selected (iso)citrate, malate, and ATP as representative metabolites for targeted analysis. While malate and ATP exhibited comparable peak areas between the two methods (Figure 7A–C), (iso)citrate showed markedly enhanced signal intensity under LT-ZHILIC conditions, indicating improved detection sensitivity. Variability assessment further underscored the advantage of LT-ZHILIC: In 10 of 12 treatment–metabolite comparisons, LT-ZHILIC yielded lower coefficients of variation (CV %) than ZIC-pHILIC (Figure 7D–F). Although we observed slightly higher CVs under specific conditions (e.g., glutamine enriched but pyruvate depleted media), LT-ZHILIC overall demonstrated comparable or superior intensity and generally higher ability to reliably quantify these metabolites, supporting its high suitability for targeted metabolomics workflows.

To further evaluate the targeted metabolomics capabilities of LT-ZHILIC, we examined NAD^+ and NADH profiles under each nutrient condition. These cofactors were selected due to their central roles in cellular redox balance and their sensitivity to metabolic perturbations. We quantified NAD^+, NADH, and their redox ratios based on peak areas obtained from both ZIC-pHILIC and LT-ZHILIC across four treatment groups (Figure 8A–C).

https://doi.org/10.1021/acs.jproteome.5c01216
J. Proteome Res. XXXX, XXX, XXX–XXX

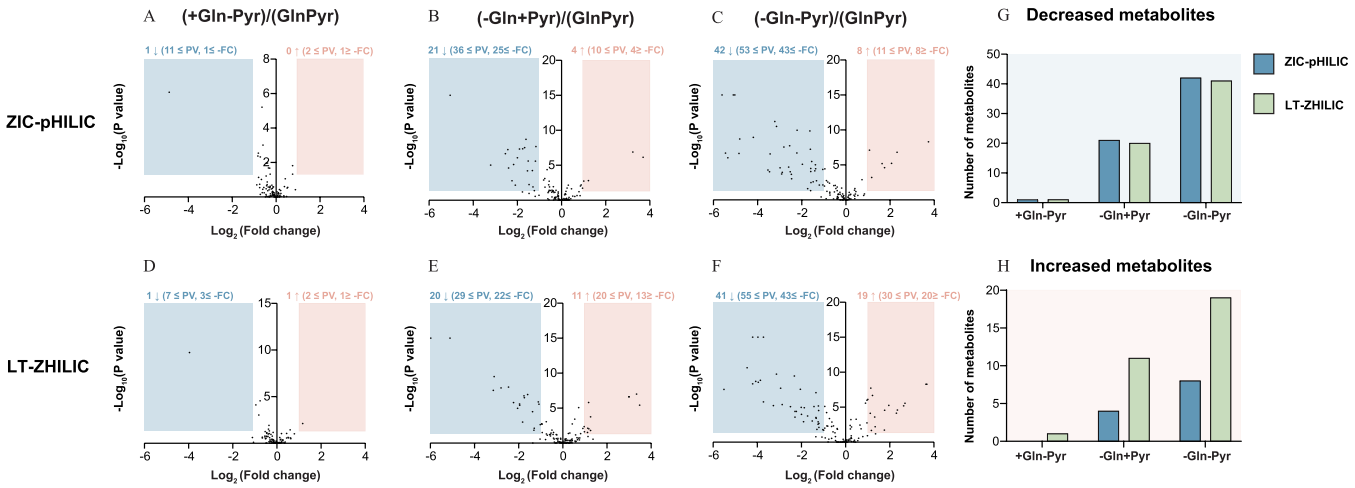

Figure 9. Negative mode volcano plots of K562 cell extracts under different treatment conditions with or without glutamine and pyruvate. Analyzed with a Compound Discoverer automated pipeline (without the library) from data acquired using ZIC-pHILIC (A–C). Corresponding results analyzed using LT-ZHILIC (D–F). (G, H) Summary of downregulated (G) and upregulated (H) metabolites detected using ZIC-pHILIC (blue) and LT-ZHILIC (green), based on searches against online metabolite libraries.

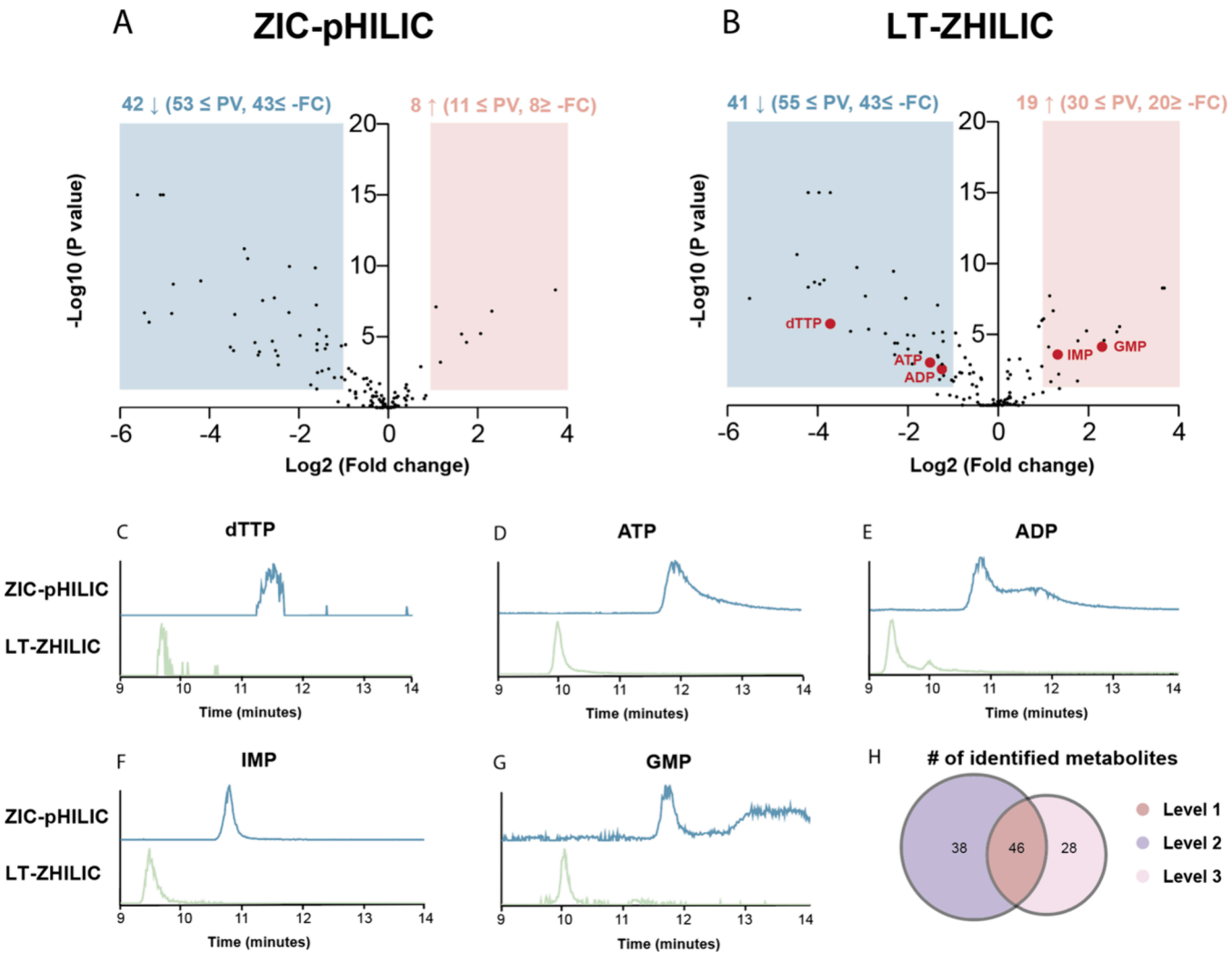

Figure 10. Nucleotide phosphate species detected in K562 cell extracts under glutamine and pyruvate deprivation, with MSI level annotation using the LT-ZHILIC library. (A, B) Volcano plots of K562 cells cultured under combined glutamine and pyruvate deprivation, analyzed in negative ion mode using ZIC-pHILIC (A) and LT-ZHILIC (B). Metabolites uniquely identified by each method are highlighted in red. (C–G) Peak shape comparisons of selected metabolites detected by LT-ZHILIC (green) and ZIC-pHILIC (blue). (H) Reanalysis of the + pyruvate/+glutamine extracts with the LT-ZHILIC method using the library resulted in 112 metabolite identifications.

https://doi.org/10.1021/acs.jproteome.5c01216
J. Proteome Res. XXXX, XXX, XXX–XXX

Absolute signal intensities for both NAD^+ and NADH were consistently higher when measured using ZIC-pHILIC compared to LT-ZHILIC across all conditions (Figure 8A,B). The calculated NAD^+/NADH redox ratios were substantially higher in ZIC-pHILIC, particularly under control conditions and in the absence of pyruvate (Figure 8C). However, the coefficient of variation (CV%) for the NAD^+/NADH ratio was also significantly higher in ZIC-pHILIC (Figure 8D), indicating reduced quantitative reproducibility compared to LT-ZHILIC. To investigate the source of these discrepancies, we directly compared chromatographic and spectral profiles of NAD^+ and NADH between the two methods. Due to their nearly identical molecular weights and similar polarity, separation of these cofactors is inherently challenging. In ZIC-pHILIC, NAD^+ and NADH coeluted, resulting in overlapping chromatographic peaks (Figure 8E) and nearly indistinguishable mass spectra (Figure 8G). The M+2 isotopic peak of NAD^+ overlapped with the M+0 peak of NADH, leading to artificially elevated NADH quantification and distorted peak shapes. In contrast, LT-ZHILIC achieved clear baseline separation of NAD^+ and NADH, producing distinct chromatographic peaks (Figure 8F) and well-resolved mass spectra (Figure 8H). This improved separation enables more accurate quantification of structurally similar redox cofactors. Together, these results demonstrate that LT-ZHILIC provides superior resolution and quantitative reliability for NAD^+/NADH analysis. In contrast, ZIC-pHILIC is prone to overestimating NAD^+ and NADH abundance and their redox ratio due to coelution and spectral overlap, potentially misrepresenting cellular redox states and associated metabolic pathways. Indeed, when NADH overestimation from M+2 isotopologue interference was quantified across four control replicates, values ranged from 46.15 to 171.79%, with ZIC-pHILIC yielding the highest overestimation at 171.79%.

Untargeted Metabolomics Analysis of Nutrient Deprivation Using LT-ZHILIC and ZIC-pHILIC

To investigate the ability of both methods to characterize metabolic alterations in cultured cells and uncover pathway-level changes, we applied untargeted metabolomics to analyze the four nutrient conditions described above. We measured the same samples in full-scan polarity-switching mode using both ZIC-pHILIC and LT-ZHILIC and used an automated Compound Discoverer pipeline, without library comparison, to analyze metabolite abundances in each condition. We generated volcano plots comparing each nutrient-deprived condition compared with control conditions (Figure 9A−F andFigure S10A−F). Overall, LT-ZHILIC identified 148 metabolites, compared with 138 detected using ZIC-pHILIC through the same pipeline. Across most treatment conditions in negative-ion mode, LT-ZHILIC detected a greater number of significantly altered metabolites ($p < 0.01$, FC >2) when glutamine and/or pyruvate were removed relative to the full-nutrient control (+Gln/+Pyr), although in some cases, both methods yielded comparable numbers of significant changes. For example, in negative ion mode, combined glutamine/pyruvate deprivation yielded only eight upregulated metabolites with ZIC-pHILIC (Figure 9C), whereas LT-ZHILIC detected 19 significantly altered metabolites under the same condition (Figure 9F). Similar trends were observed across other treatments as well as positive mode (Figure 9A,B,D,Eand Figure S10A−F), where LT-ZHILIC consistently detected more significant metabolite changes than ZIC-pHILIC (Figure 9G,H andFigure S10G,H). The exact mechanism underlying these differences between the two columns remains unclear. It is possible that LT-ZHILIC provides improved fragmentation or more consistent elution profiles, which, when analyzed with the same metabolomics pipeline, resulted in a higher number of detected metabolites.

We next performed a focused analysis of the significantly altered metabolites in negative ion mode under combined glutamine and pyruvate deprivation. Several nucleotide phosphate species—including dTTP, ATP, ADP, IMP, and GMP—showed significant alterations only when analyzed using LT-ZHILIC (highlighted in red), whereas they were not identified in ZIC-pHILIC analyses (Figure 10A,B). Interestingly, ATP from ZIC-pHILIC was not found with the automated metabolite identification pipeline, despite exhibiting a peak shape sufficient for targeted quantitation (Figure 7C,F). To further investigate the source of this improved performance, we compared the peak shapes of nucleotide phosphates across both methods (Figure 10C−G). Chromatograms show that LT-ZHILIC (green traces) yields sharper and more symmetrical peaks than ZIC-pHILIC (blue traces). However, despite observing clear peaks for all five metabolites from ZIC-pHILIC, our automated analysis pipeline with Compound Discoverer was unable to identify these metabolites. We hypothesize that these nucleotide phosphates were detectable only with LT-ZHILIC because this method provides improved signal-to-noise ratios and substantially narrower elution profiles. For example, ATP exhibited a marked reduction in full peak width from 3.35 ± 0.09 min with ZIC-pHILIC to 0.81 ± 0.13 min with LT-ZHILIC, supporting this interpretation. Collectively, these results underscore the ability of LT-ZHILIC to deliver deep biological insights through enhanced sensitivity, improved peak shapes, and broader metabolic coverage.

We subsequently searched the results from + glutamine + pyruvate against the LT-ZHILIC library to demonstrate potential future applications to cell extracts. Metabolite identification was assigned according to MSI confidence levels (Figure10H). In negative ion mode, 46 metabolites were identified at MSI level 1 (matching retention time and MS/MS), 84 at level 2 (MS/MS only), and 74 at level 3 (retention time only). Collectively, these results demonstrate that coupling LT-ZHILIC with a library of standard metabolites enables high sensitivity and confidence in untargeted metabolite identification.

DISCUSSION

Since its introduction by Waters,[16] the Z-HILIC column has been applied to metabolomics studies[27,28] and is generally used with the ABC B gradient system. However, to our knowledge, no prior reports have systematically described the retention time drift associated with the ABC B system, which can potentially bias quantitative metabolomics results. One previous study observed peak pattern shifts when using standard borosilicate glass bottles and attributed these changes to ion leaching (e.g., sodium, potassium, and borate) that altered the mobile phase composition.[25] Although that study demonstrated improved short-term stability (up to 12 h) using plastic solvent bottles, our experiments (Figure S1) demonstrated that this modification did not fully resolve the issue. In our hands, the ABC B mobile phase exhibited progressive retention time drift over 4 days, consistent with the chemical instability of ammonium bicarbonate. This buffer gradually

https://doi.org/10.1021/acs.jproteome.5c01216
J. Proteome Res. XXXX, XXX, XXX−XXX

decomposes into ammonia, carbon dioxide, and water at room temperature, leading to the loss of volatile components, pH drift, and reduced buffering capacity.[29] Although quaternary pumping systems could, in principle, mitigate some retention challenges by enabling more flexible solvent blending, they are known to exhibit poor reproducibility under the shallow-gradient conditions required for comprehensive metabolome profiling. In mixed aqueous−organic systems, additional factors such as limited solubility and solvent evaporation further accelerate degradation, contributing to signal variability and migration of chromatographic peaks. By contrast, the alternative ACN B method showed no retention drift but yielded poorer chromatographic resolution, highlighting a trade-off between stability and separation performance.

Building on previous studies, modulation of column temperature can significantly improve HILIC separations, with the optimal conditions depending on the specific analytes of interest.[28,30] We found substantial improvement to ACN B by operating with the column compartment at 5 °C. Low-temperature operation, though commonly used in hydrogen−deuterium (HDX) exchange mass spectrometry (MS) to preserve labile features and prevent back-exchange,[31] has rarely been applied in metabolomics, where higher temperatures (typically around or above 30 °C) are favored to improve peak shape and reproducibility.[18,7] However, we observed that at these higher temperatures, key metabolites such as (iso)citrate, malate, and ATP often produce broad or poorly resolved elution profiles, thereby limiting detection sensitivity and metabolome coverage in untargeted analyses. In addition, redox-active and nucleotide phosphate metabolites are particularly prone to artifactual noise or quantification bias when analyzed using standard methods such as ZIC-pHILIC.[32,33] By contrast, here we show that LT-ZHILIC produced sharper, more symmetrical peaks for several selected metabolites, by coupling with an in-house-made library resulting in higher quantitative reliability and stability for both targeted and untargeted analyses. While the precise mechanism remains to be fully established, several factors may contribute to the observed effect. In HILIC separations, analyte retention is generally governed by partitioning between the organic rich mobile phase and a water enriched interfacial layer associated with the stationary phase.[34] Lower column temperatures may stabilize this interfacial water layer and reduce analyte diffusion, leading to more uniform analyte interactions with the stationary phase and reduced peak broadening. We further found that it is the inherent column temperature and not the temperature difference between buffers and column that drive the effect (Figure S9A−F).

Interestingly, lowering the column temperature did not improve peak shapes when the same approach was applied to a ZIC-pHILIC column. This difference may reflect the distinct stationary phase chemistries of the two materials. ZIC-pHILIC columns employ a polymeric stationary phase, while Z-HILIC columns are based on bridged ethylene hybrid (BEH) particles, which emphasize partition-dominated retention mechanisms.[35] Interestingly, we noted decreased RT time at low temperatures for the LT-ZHILIC and ZIC-pHILIC columns with zwitterionic stationary phases, suggesting weaker retention of compounds at cold temperature. The opposite trend was observed for the BEH Amide column. Temperature-dependent changes in interfacial water structure and diffusion behavior may therefore influence differently stationary phases depending on BEH vs polymeric support and zwitterionic vs amide functional groups. In addition to chromatographic improvements, operating at lower column temperatures may also improve the stability of certain labile metabolites, although this possibility remains speculative and will require further investigation.

Building on the demonstrated stability of LT-ZHILIC, the accompanying LT-ZHILIC library enabling up to MSI level 1 identification further enhances confidence in metabolite annotation for both standards and complex biological samples. Our findings demonstrate that LT-ZHILIC generally outperforms ZIC-pHILIC in resolving biologically relevant metabolites, particularly those involved in energy metabolism, redox regulation, and nucleotide turnover. The NAD^+/NADH ratio is a master regulator of cellular redox homeostasis, governing mitochondrial respiration, oxidative stress signaling, and the activity of numerous metabolic enzymes.[36]

Therefore, the systematic overestimation observed with ZIC-pHILIC introduces a significant risk of misinterpreting redox dynamics due to its high variability. Likewise, nucleotide phosphates such as ATP, ADP, and AMP are foundational to energy transfer, kinase signaling, and metabolic flux; failure to detect ATP in an untargeted workflow, as observed with ZIC-pHILIC, can fundamentally distort interpretation of cellular energy states.[37] In contrast, LT-ZHILIC consistently captures these key metabolites with high fidelity using the same analysis pipeline, providing a markedly more reliable representation of underlying biology. While the mechanistic basis for its enhanced performance warrants further investigation, the evidence presented here establishes LT-ZHILIC as the more robust and biologically accurate platform for metabolomics studies requiring precise quantification of redox and energy-related metabolites.

While the LT-ZHILIC method offers substantial improvements in chromatographic stability and performance, several limitations remain. Proper maintenance and thorough equilibration are strongly recommended. For a fresh column, we recommend running 10 column volumes of 20% mobile phase A and 80% mobile phase B, followed by an additional 10 blank injections prior to the actual analysis. Moreover, operation at low temperatures (≈5 °C) is not universally compatible with all LC systems and may require external temperature-control setups, such as the customized chamber used in our cryogenic experiments. Another area for improvement is the coverage of the LT-ZHILIC library, which can be expanded to include more annotated metabolites to enhance its applicability across a broader range of analytical workflows and sample types. Finally, although the LT-ZHILIC system demonstrated stable retention over the tested time period and supports large batches of samples, longer-term evaluations are still needed to fully assess its robustness for extended studies and high-throughput metabolomics workflows. The method can also be applied to other LC platforms; however, further optimization may be required for specific instrument configurations. Collectively, these findings indicate that while LT-ZHILIC represents a promising advancement, additional optimization and method development will be important for its broader adoption.

CONCLUSIONS

In this study, we characterized two buffer systems for chromatographic LC-MS separation of plasma and intracellular extracts on a Z-HILIC column and found that using high-pH ammonium bicarbonate in buffer B can substantially improve

https://doi.org/10.1021/acs.jproteome.5c01216
J. Proteome Res. XXXX, XXX, XXX−XXX

peak shapes, but at the cost retention time drift over the course of 4 days. We therefore introduce an optimized low-temperature (5 °C) HILIC approach (LT-ZHILIC), which uses only acetonitrile in buffer B and exhibits improved peak shapes and robust retention time stability. We further established an LT-ZHILIC-coupled metabolite library covering a broad range of metabolites to enhance its applicability in metabolomics identification. Notably, LT-ZHILIC demonstrated high resolution in targeted analyses of TCA cycle intermediates and redox-sensitive metabolites (e.g., NAD^+ and NADH), as well as in untargeted analysis of nucleotide phosphates. Compared with the commonly used ZIC-pHILIC method, LT-ZHILIC performed equivalently or better, reducing analytical variability and enabling more reliable quantitative measurements in untargeted metabolomics. Collectively, these results establish LT-ZHILIC as a robust and versatile chromatographic platform, highlighting its potential to uncover previously obscured biochemical changes and to support future pathway focused and therapeutic investigations.

■ ASSOCIATED CONTENT

Data Availability Statement

All data supporting the findings of this study are available within the manuscript and its Supporting Information. Raw data files are publicly available via MassIVE (identifier: MSV000100254). The data have been organized to ensure transparency and facilitate reuse by other researchers.

Supporting Information

The Supporting Information is available free of charge at https://pubs.acs.org/doi/10.1021/acs.jproteome.5c01216.

(Figure S1) Retention time stability of succinate with ABC B and ACN B, and selected metabolites from K562 cell extracts analyzed using mobile phase stored in plastic bottles; (Figure S2) column compartment setup for cryogenic HILIC; (Figure S3) optimization of the ABC B method under low-temperature conditions (Cryo-HILIC); (Figure S4) retention time stability of LT-ZHILIC; (Figure S5) retention time stability of metabolites in K562 cell and plasma extracts over 4 and 11 days; (Figure S6) reproducibility of chromatographic performance across multiple injections; (Figure S7) peak shape comparison of selected metabolites analyzed on a Waters M-class ACQUITY UPLC coupled to a SYNAPT G2-Si mass spectrometer; (Figure S8) peak shape comparison between LT-ZHILIC and ZIC-pHILIC; (Figure S9) effects of column and mobile phase temperature on metabolite separation; and (Figure S10) positive mode volcano plots of K562 cell extracts under different treatment conditions with or without glutamine and pyruvate (PDF)

List of metabolites identified in both negative and positive ion modes in the LT-ZHILIC library (XLSX)

■ AUTHOR INFORMATION

Corresponding Author

Owen S. Skinner − *Department of Chemistry and Chemical Biology, Northeastern University, Boston, Massachusetts 02115, United States;* orcid.org/0000-0002-5023-0029; Email: o.skinner@northeastern.edu

Authors

Yifan Liu − *Department of Chemistry and Chemical Biology, Northeastern University, Boston, Massachusetts 02115, United States*

Madison L. Jastrab − *Department of Chemistry and Chemical Biology, Northeastern University, Boston, Massachusetts 02115, United States*

Michael Xiao − *Department of Chemistry and Chemical Biology, Northeastern University, Boston, Massachusetts 02115, United States*

Miriam Lisci − *Department of Immunobiology, Faculty of Biology and Medicine, University of Lausanne, Lausanne 1015, Switzerland*

Bindu Y. Srinivasu − *Department of Chemistry and Chemical Biology, Northeastern University, Boston, Massachusetts 02115, United States*

Taysir K. Bader − *Waters Corporation, Milford, Massachusetts 01757, United States*

Alexis A. Jourdain − *Department of Immunobiology, Faculty of Biology and Medicine, University of Lausanne, Lausanne 1015, Switzerland*

Thomas E. Wales − *Department of Chemistry and Chemical Biology, Northeastern University, Boston, Massachusetts 02115, United States*

Complete contact information is available at: https://pubs.acs.org/10.1021/acs.jproteome.5c01216

Notes

The authors declare the following competing financial interest(s): O.S.S. served as a consultant for Handshake AI. T.K.B. is an employee at Waters.

■ ACKNOWLEDGMENTS

We would like to thank Dr. Alexander Ivanov, Purvi Saxena, and Angela Rojas-Merchan for helpful discussions. Images in the TOC were created with BioRender (biorender.com).

■ REFERENCES

(1) Pathmasiri, W.; Rushing, B. R.; McRitchie, S.; Choudhari, M.; Du, X.; Smirnov, A.; Pelleigrini, M.; Thompson, M. J.; Sakaguchi, C. A.; Nieman, D. C.; Sumner, S. J. Untargeted Metabolomics Reveal Signatures of a Healthy Lifestyle. *Sci. Rep.* **2024**, *14* (1), 13630.

(2) Bundy, J. G.; Davey, M. P.; Viant, M. R. Environmental Metabolomics: A Critical Review and Future Perspectives. *Metabolomics* **2009**, *5* (1), 3−21.

(3) Jeppesen, M. J.; Powers, R. Multiplatform Untargeted Metabolomics. *Magn. Reson. Chem. MRC* **2023**, *61* (12), 628−653.

(4) Gagnebin, Y.; Julien, B.; Belén, P.; Serge, R. Metabolomics in Chronic Kidney Disease: Strategies for Extended Metabolome Coverage. *J. Pharm. Biomed. Anal.* **2018**, *161*, 313−325.

(5) Xu, Z.; Zhou, Y.; Xie, R.; Ning, Z. Metabolomics Uncovers the Diabetes Metabolic Network: From Pathophysiological Mechanisms to Clinical Applications. *Front. Endocrinol.* **2025**, *16*, No. 1624878.

(6) Theodoridis, G.; Gika, H.; Raftery, D.; Goodacre, R.; Plumb, R. S.; Wilson, I. D. Ensuring Fact-Based Metabolite Identification in Liquid Chromatography-Mass Spectrometry-Based Metabolomics. *Anal. Chem.* **2023**, *95* (8), 3909−3916.

(7) Abdelrazig, S.; McCabe, Á.; Yasin, A.; Chaudhary, R.; Ochsenkühn, M. A.; Scicchitano, D.; Amin, S. A. LC-MS Orbitrap-Based Metabolomics Using a Novel Hybrid Zwitterionic Hydrophilic Interaction Liquid Chromatography and Rigorous Metabolite Identification Reveals Doxorubicin-Induced Metabolic Perturbations in Breast Cancer Cells. *RSC Adv.* **2025**, *15* (26), 20745−20759.

(8) *A complete workflow for high-resolution spectral-stitching nano-electrospray direct-infusion mass-spectrometry-based metabolomics and lipidomics | Springer Nature Experiments*. https://experiments.springernature.com/articles/10.1038/nprot.2016.156 (accessed 2025−10−30).
(9) Dunn, W. B.; Broadhurst, D.; Begley, P.; Zelena, E.; Francis-McIntyre, S.; Anderson, N.; Brown, M.; Knowles, J. D.; Halsall, A.; Haselden, J. N.; Nicholls, A. W.; Wilson, I. D.; Kell, D. B.; Goodacre, R. Procedures for Large-Scale Metabolic Profiling of Serum and Plasma Using Gas Chromatography and Liquid Chromatography Coupled to Mass Spectrometry. *Nat. Protoc.* **2011**, *6* (7), 1060−1083.
(10) Naser, F. J.; Mahieu, N. G.; Wang, L.; Spalding, J. L.; Johnson, S. L.; Patti, G. J. Two Complementary Reversed-Phase Separations for Comprehensive Coverage of the Semipolar and Nonpolar Metabolome. *Anal. Bioanal. Chem.* **2018**, *410* (4), 1287−1297.
(11) Exploring the Dual Retention Mechanism of Mixed-Mode Acclaim WAX-1 Columns to Tune Selectivity in Liquid Chromatography.
(12) Rojo, D.; Barbas, C.; Rupérez, F. J. LC-MS Metabolomics of Polar Compounds. *Bioanalysis* **2012**, *4* (10), 1235−1243.
(13) Cubbon, S.; Antonio, C.; Wilson, J.; Thomas-Oates, J. Metabolomic Applications of HILIC-LC-MS. *Mass Spectrom. Rev.* **2010**, *29* (5), 671−684.
(14) Xu, Y.; Heilier, J.-F.; Madalinski, G.; Genin, E.; Ezan, E.; Tabet, J.-C.; Junot, C. Evaluation of Accurate Mass and Relative Isotopic Abundance Measurements in the LTQ-Orbitrap Mass Spectrometer for Further Metabolomics Database Building. *Anal. Chem.* **2010**, *82* (13), 5490−5501.
(15) Boersema, P. J.; Mohammed, S.; Heck, A. J. R. Hydrophilic Interaction Liquid Chromatography (HILIC) in Proteomics. *Anal. Bioanal. Chem.* **2008**, *391* (1), 151−159.
(16) *Introducing Atlantis BEH Z-HILIC: A Zwitterionic Stationary Phase Based on Hybrid Organic/Inorganic Particles*. https://www.waters.com/nextgen/us/en/library/application-notes/2021/introducing-atlantis-beh-z-hilic-a-zwitterionic-stationary-phase-based-on-hybrid-organic-inorganic-particles.html (accessed 2025−10−30).
(17) Contrepois, K.; Jiang, L.; Snyder, M. Optimized Analytical Procedures for the Untargeted Metabolomic Profiling of Human Urine and Plasma by Combining Hydrophilic Interaction (HILIC) and Reverse-Phase Liquid Chromatography (RPLC)−Mass Spectrometry*. *Mol. Cell. Proteomics* **2015**, *14* (6), 1684−1695.
(18) Hosseinkhani, F.; Huang, L.; Dubbelman, A.-C.; Guled, F.; Harms, A. C.; Hankemeier, T. Systematic Evaluation of HILIC Stationary Phases for Global Metabolomics of Human Plasma. *Metabolites* **2022**, *12* (2), 165.
(19) DeLano, M.; Walter, T. H.; Lauber, M. A.; Gilar, M.; Jung, M. C.; Nguyen, J. M.; Boissel, C.; Patel, A. V.; Bates-Harrison, A.; Wyndham, K. D. Using Hybrid Organic−Inorganic Surface Technology to Mitigate Analyte Interactions with Metal Surfaces in UHPLC. *Anal. Chem.* **2021**, *93* (14), 5773−5781.
(20) *Separation of Pentose Phosphate Pathway, Glycolysis, and Energy Metabolites Using an ACQUITY Premier System With an Atlantis Premier BEH Z-HILIC Column*. https://www.waters.com/nextgen/us/en/library/application-notes/2021/separation-of-pentose-phosphate-pathway-glycolysis-and-energy-metabolites-using-an-acquity-premier-system-with-an-atlantis-premier-beh-z-hilic-column.html (accessed 2025−10−30).
(21) Skinner, O. S.; Blanco-Fernández, J.; Goodman, R. P.; Kawakami, A.; Shen, H.; Kemény, L. V.; Joesch-Cohen, L.; Rees, M. G.; Roth, J. A.; Fisher, D. E.; Mootha, V. K.; Jourdain, A. A. Salvage of Ribose from Uridine or RNA Supports Glycolysis in Nutrient-Limited Conditions. *Nat. Metab.* **2023**, *5* (5), 765−776.
(22) Salek, R. M.; Steinbeck, C.; Viant, M. R.; Goodacre, R.; Dunn, W. B. The Role of Reporting Standards for Metabolite Annotation and Identification in Metabolomic Studies. *GigaScience* **2013**, *2*, 13.
(23) Lu, W.; Wang, L.; Chen, L.; Hui, S.; Rabinowitz, J. D. Extraction and Quantitation of Nicotinamide Adenine Dinucleotide Redox Cofactors. *Antioxid. Redox Signal.* **2018**, *28* (3), 167−179.
(24) Wales, T. E.; Fadgen, K. E.; Gerhardt, G. C.; Engen, J. R. High-Speed and High-Resolution UPLC Separation at Zero Degrees Celsius. *Anal. Chem.* **2008**, *80* (17), 6815−6820.
(25) Serafimov, K.; Knappe, C.; Li, F.; Sievers-Engler, A.; Lämmerhofer, M. Solving the Retention Time Repeatability Problem of Hydrophilic Interaction Liquid Chromatography. *J. Chromatogr. A* **2024**, *1730*, No. 465060.
(26) Mick, E.; Titov, D. V.; Skinner, O. S.; Sharma, R.; Jourdain, A. A.; Mootha, V. K. Distinct Mitochondrial Defects Trigger the Integrated Stress Response Depending on the Metabolic State of the Cell. *eLife* **2020**, *9*, No. e49178.
(27) Nakatani, K.; Izumi, Y.; Takahashi, M.; Bamba, T. Unified-Hydrophilic-Interaction/Anion-Exchange Liquid Chromatography Mass Spectrometry (Unified-HILIC/AEX/MS): A Single-Run Method for Comprehensive and Simultaneous Analysis of Polar Metabolome. *Anal. Chem.* **2022**, *94* (48), 16877−16886.
(28) Zhang, R.; Watson, D. G.; Wang, L.; Westrop, G. D.; Coombs, G. H.; Zhang, T. Evaluation of Mobile Phase Characteristics on Three Zwitterionic Columns in Hydrophilic Interaction Liquid Chromatography Mode for Liquid Chromatography-High Resolution Mass Spectrometry Based Untargeted Metabolite Profiling of *Leishmania* Parasites. *J. Chromatogr. A* **2014**, *1362*, 168−179.
(29) Hedges, J. B.; Vahidi, S.; Yue, X.; Konermann, L. Effects of Ammonium Bicarbonate on the Electrospray Mass Spectra of Proteins: Evidence for Bubble-Induced Unfolding. *Anal. Chem.* **2013**, *85* (13), 6469−6476.
(30) *Impact of column temperature and mobile phase components on selectivity of hydrophilic interaction chromatography (HILIC)*.. .
(31) Tajoddin, N. N.; Konermann, L. Analysis of Temperature-Dependent H/D Exchange Mass Spectrometry Experiments. *Anal. Chem.* **2020**, *92* (14), 10058−10067.
(32) Spalding, J. L.; Naser, F. J.; Mahieu, N. G.; Johnson, S. L.; Patti, G. J. Trace Phosphate Improves ZIC-pHILIC Peak Shape, Sensitivity, and Coverage for Untargeted Metabolomics. *J. Proteome Res.* **2018**, *17* (10), 3537−3546.
(33) Sutton, T. R.; Minnion, M.; Barbarino, F.; Koster, G.; Fernandez, B. O.; Cumpstey, A. F.; Wischmann, P.; Madhani, M.; Frenneaux, M. P.; Postle, A. D.; Cortese-Krott, M. M.; Feelisch, M. A Robust and Versatile Mass Spectrometry Platform for Comprehensive Assessment of the Thiol Redox Metabolome. *Redox Biol.* **2018**, *16*, 359−380.
(34) McCalley, D. V.*Hydrophilic-Interaction Chromatography: An Update | LCGC International*. https://www.chromatographyonline.com/view/hydrophilic-interaction-chromatography-update?utm_source=chatgpt.com (accessed 2026−03−30).
(35) Ntorkou, M.; Zacharis, C. K. Applications of Hydrophilic Interaction Chromatography in Pharmaceutical Impurity Profiling: A Comprehensive Review of Two Decades. *Molecules* **2025**, *30* (17), 3567.
(36) Titov, D. V.; Cracan, V.; Goodman, R. P.; Peng, J.; Grabarek, Z.; Mootha, V. K. Complementation of Mitochondrial Electron Transport Chain by Manipulation of the NAD+/NADH Ratio. *Science* **2016**, *352* (6282), 231−235.
(37) Ryu, K. W.; Fung, T. S.; Baker, D. C.; Saoi, M.; Park, J.; Febres-Aldana, C. A.; Aly, R. G.; Cui, R.; Sharma, A.; Fu, Y.; Jones, O. L.; Cai, X.; Pasolli, H. A.; Cross, J. R.; Rudin, C. M.; Thompson, C. B. Cellular ATP Demand Creates Metabolically Distinct Subpopulations of Mitochondria. *Nature* **2024**, *635* (8039), 746−754.

https://doi.org/10.1021/acs.jproteome.5c01216
J. Proteome Res. XXXX, XXX, XXX−XXX